ISSN 0965-545X, Polymer Science, Ser. A, 2012, Vol. 54, No. 8, pp. 631–643. © Pleiades Publishing, Ltd., 2012.
Original Russian Text © S.V. Lyulin, S.V. Larin, A.A. Gurtovenko, N.V. Lukasheva, V.E. Yudin, V.M. Svetlichnyi, A.V. Lyulin, 2012, published in Vysokomolekulyarnye Soedineniya, Ser. A, 2012, Vol. 54, No. 8, pp. 1253–1266.

Effect of the SO_2 Group in the Diamine Fragment of Polyimides on Their Structural, Thermophysical, and Mechanical Properties[1]

S. V. Lyulin[a, b]*, S. V. Larin[a], A. A. Gurtovenko[a, b], N. V. Lukasheva[a], V. E. Yudin[a], V. M. Svetlichnyi[a], and A. V. Lyulin[c]

[a] *Institute of Macromolecular Compounds, Russian Academy of Sciences, Bol'shoi pr. 31 (V.O.), St. Petersburg, 199004 Russia*
[b] *Faculty of Physics, St. Petersburg State University, Ul'yanovskaya ul. 1, Petrodvorets, St. Petersburg, 198504 Russia*
[c] *Department of Applied Physics, Eindhoven University of Technology, P.O Box 513 5600 MB Eindhoven, Netherlands*
**e-mail: s.v.lyulin@gmail.com*

Received November 29, 2011;
Revised Manuscript Received January 23, 2012

Abstract—Experimental and theoretical investigations, including an all-atom computer simulation, are performed for block samples of thermoplastic polyimides, amorphous R-BAPS (based on R dianhydride 1,3-bis(3',4-dicarboxyphenoxy)benzene and diamine BAPS 4,4'-bis(4''-aminophenoxy)biphenyl sulfone), and crystallizable R-BAPB (based on R dianhydride and diamine BAPB 4,4'-bis(4''-aminophenoxy)biphenyl), which differ in either the presence or absence of the sulfone group in the repeating unit of the polyimide macromolecule. The features of thermophysical, structural, and mechanical properties of R-BAPS and R-BAPB are related to the formation of associates from sulfur and oxygen atoms of the sulfone group that are stabilized by electrostatic interactions.

DOI: 10.1134/S0965545X12070048

INTRODUCTION

Aromatic polyimides (PIs) belong to the class of thermostable polymers that have found wide use in numerous fields of modern engineering [1]. However, the industrial production of polyimides is restrained because the processing of these materials into articles is problematic. These polymers are typically unmeltable and insoluble in the most commonly used organic solvents. The emergence of the subgroup of poly(ether imides)—polymers that are capable of being processed from melt and in which imide aromatic groups are separated from each other by ether bonds—in the PI class is a significant advance in the chemistry and technology of condensation polymers [2–4]. The industrial fabrication of poly(ether imide) (ULTEM®) was launched by the General Electric Company in 1986 on the basis of studies of a number of poly(ether imides) [5, 6]. Today, this poly(ether imide) is in wide use in the engineering and electronic industries as well as in aircraft and space engineering. In 2007, General Electric produced a new poly(ether imide) (EXTEM®) with a higher glass-transition temperature: For ULTEM® T_g = 491 K (218°C) [7], whereas for EXTEM®, T_g = 540 K (267°C) [8] (Table 1). Furthermore, EXTEM® features exceptional size stability, high strength, rigidity, high-temperature creep resistance, and incombustibility [9]. The production rights for this polymer currently belong to the company SABIC Innovative Plastics^{tm}.

Although the polyimides ULTEM® and EXTEM® have identical dianhydride fragments in the structural formulas of their repeating units, the structures of diamine fragments in these polymers are different [9].

Table 1. Comparison of the experimental glass-transition temperatures obtained from the QSPR analysis and computer simulation results

Polymer	T_g, K		
	Experiment	QSPR	Simulation
R-BAPB	477 according to [22]	468.7	472–476
R-BAPS	490 according to [22]	516.4	494–496
ULTEM	491 according to [7]	493.3	–
EXTEM	540 according to [8]	538.5	–

[1] This work was supported by the Russian Foundation for Basic Research (project no. 11-03-00944-a) and the Ministry of Education and Science of the Russian Federation (State Contact no. 16.523.12.3001).

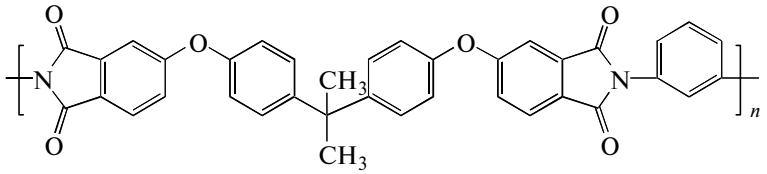

ULTEM®

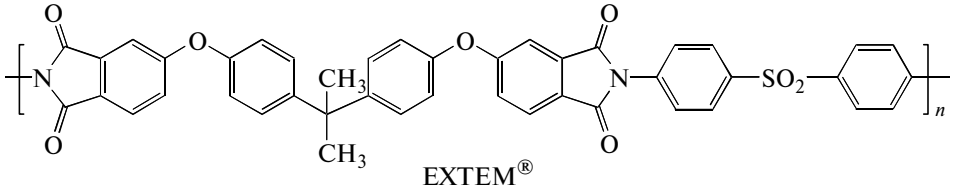

EXTEM®

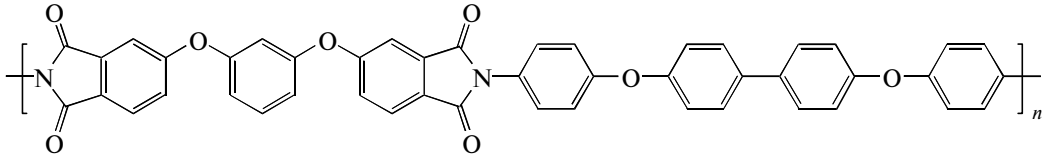

R-BAPB

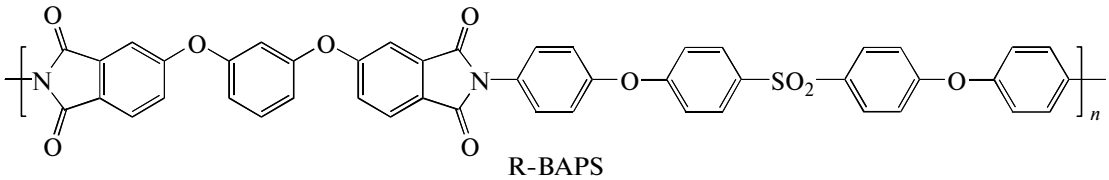

R-BAPS

In the diamine fragment of EXTEM®, there is an SO_2 hinge group between benzene rings. This modification is responsible for a considerable difference in the thermophysical characteristics of ULTEM® and EXTEM® [7, 8, 10].

The wide application of ULTEM® and EXTEM® polyimides makes it necessary to elucidate the effect of insertion of the heteroatomic SO_2 group into the diamine fragment of the repeating PI unit on the fragment's structural, thermophysical, and mechanical properties. This knowledge will enable fabrication of similar materials with enhanced properties that are based on other monomers.

QSPR ANALYSIS

A wide range of characteristics of ULTEM® and EXTEM® were compared via the QSPR (Quantitative Structure–Property Relationships) analysis of the chemical structures of repeating units with the use of the SYNTHIA module (Material Studio 5.5 software package) [11]. This analysis makes it possible to assess the properties of block amorphous homopolymers on the basis of structural formula of their repeating units. The relevant data are summarized in Table 2. It is clear that the insertion of sulfur and oxygen heteroatoms into the diamine component of the repeating EXTEM® unit results in a considerable alteration in the density, the glass-transition temperature, and other characteristics. However, some characteristics remain unchanged. Thus, QSPR analysis demonstrates that thermal conductivity and the Poisson coefficient remain invariable.

A comparison of the glass-transition temperature (Table 1) obtained via the QSPR analysis with the known experimental data [7, 8] for ULTEM® and EXTEM® provides good agreement, which attests to the significance of these predictions. However, the QSPR analysis cannot explain the mechanism of changes in physical properties of ULTEM® as compared to EXTEM®; i.e., when a hinge group containing sulfur and oxygen heteroatoms is inserted into the diamine PI unit. In this study, an attempt was made not only to ascertain this mechanism on the basis of atomistic computer simulation of other polyimide thermoplastics that can be used to produce new thermostable composites but also to validate this simulation through comparison of the results with experimental data.

SYNTHESIS

PIs based on 1,3-bis(3',4-dicarboxyphenoxy)benzene (dianhydride R) and diamines of two types—4,4'-bis(4''-aminophenoxy)biphenyl sulfone (BAPS diamine) and 4,4'-bis(4''-aminophenoxy)biphenyl (BAPB diamine)—were selected as thermoplastic polyimide matrices that can be processed via melt technology (extrusion, casting). These PIs were developed at the Institute of Macromolecular Compounds of the Russian Academy of Sciences [12–22] and were selected, first, owing to the high potential of their use

Table 2. Some physical characteristics of PIs at room temperature (290 K) obtained from the data of the QSPR analysis

Polyimide	M_w (8 repeating units), g/mol	M_w of the repeating unit, g/mol	Length of the repeating unit, Å	T_g, K	$\beta \times 10^{-6}$, K^{-1}	Molar volume*	Density*, kg/m^3	Thermal conductivity, W/(m K)	Permittivity at 298 K
R-BAPB	5882	734.7	34.0	468.7	211.1	563.0/563.9	1.31/1.30	0.2	3.22
R-BAPS	6394	798.8	34.6	516.4	192.8	589.3/590.2	1.36/1.35	0.2	3.50
ULTEM®	4746	592.6	23.4	493.3	201.2	462.6/463.3	1.28/1.28	0.2	3.23
EXTEM®	5866	732.8	28.6	538.5	185.3	555.3/556.1	1.32/1.32	0.2	3.46

Polyimide	Bulk modulus, GPa	Shear modulus, GPa	Young's modulus, GPa	Poisson coefficient	Average M_w of the polymer between entanglements	Average polymer length between entanglements, Å	Average polymer length between entanglements (number of repeating units)
R-BAPB	5.412	1.035	2.918	0.41	2095	96.85	2.85
R-BAPS	6.107	1.191	3.355	0.41	2289	99.14	2.87
ULTEM®	5.492	1.163	3.258	0.40	2583	102.14	4.36
EXTEM®	6.083	1.282	3.592	0.40	2634	102.72	3.59

Note: * The parameter values in the numerator and denominator are given at 290 and 298 K, respectively.

as thermoplastic binding agents for composite materials [12–21] and, second (as in the case of the ULTEM®–EXTEM® pair) owing to the possibility of studying the effect of the SO_2 group in the diamine fragment of the repeating unit of the R-BAPS polyimide on its structural, thermophysical, and mechanical properties relative to the effect of the SO_2 group in the diamine fragment of the repeating unit of the R-BAPB polyimide on its structural, thermophysical, and mechanical properties. An additional advantage of R-BAPB is that it can crystallize. However, only amorphous samples were investigated in this study.

R-BAPS and R-BAPB polyimides were prepared via the conventional two-stage procedure [1]. At the first stage, the poly(amido acid) is formed in an *N*-methylpyrrolidone (MP) solution. A stoichiometric amount of 1,3-bis(3',4-dicarboxyphenoxy)benzene dianhydride was added to a stirred solution of 4,4'-bis(4''-aminophenoxy)biphenyl sulfone or to a solution of 4,4'-bis(4''-aminophenoxy)biphenyl at 20°C. The concentration of the poly(amido acid) solutions was 20 wt %; the duration of synthesis in MP was 4 h. The solution of the poly(amido acid) was applied onto a glass substrate to obtain film samples after drying (80°C, 12 h). The imidization of film samples of poly(amido acids) was performed via heating to 280°C with an exposure time of 30 min at 100, 120, 160, 200, 250, and 280°C.

THEORETICAL ASSESSMENT OF THE FLEXIBILITY OF R-BAPB AND R-BAPS MOLECULES

As was demonstrated in [12–22], R-BAPB and R-BAPS are exceptionally promising for the design of polymer composites (including nanocomposites) via melt technology. The difference in the structures of the repeating units of R-BAPB and R-BAPS polyimides (similar to that in the case of ULTEM® and EXTEM®) is that the diamine fragment of R-BAPS contains the SO_2 hinge group. However, unlike in the case of EXTEM® the number of benzene rings in the diamine component remains unchanged in R-BAPS relative to R-BAPB. This chemical modification of the repeating unit of R-BAPB, which should have facilitated an increase in the flexibility of the PI chain and a decrease in the glass-transition temperature, results in this case in an increase in the glass transition temperature, as was observed experimentally (Table 1).

In addition, the physical properties of the selected PIs were preliminarily assessed through the QSPR analysis (Table 2). For both ULTEM® and R-BAPB, the addition of the SO_2 hinge group into the diamine

Table 3. Virtual-bond lengths and valence angles in R-BAPS (Here and in Tables 4–6, *i* is the order number of a virtual bond.)

i	1	2	3	4	5	6	7	8	9	10	11	12	13	14
l	4.67	1.39	2.79	2.79	1.39	4.67	1.41	4.19	1.38	4.47	4.47	1.38	1.397	4.21
θ°	154.2	117.2	120	117.2	154.2	171.5	178.2	121.2	179	101.3	178.7	117.2	174.4	171.3

fragment clearly results in similar changes. A more thorough analysis of the mechanical properties and other data obtained via the QSPR analysis will be the subject of forthcoming papers.

As was shown by the QSPR analysis (Table 2), the flexibility of PIs examined in terms of the mean value of monomer units between entanglements is in fact identical for R-BAPB and R-BAPS, although in the latter case this value decreases slightly.

In order to assess the flexibility of R-BAPB and R-BAPS polyimides, their persistence lengths were analytically calculated [23]. The models of the repeating PI unit in conformations corresponding to the intramolecular-energy minimum for R-BAPS and R-BAPB, which were calculated via the AM1 semiempirical quantum-chemistry method, are given below.

R-BAPS

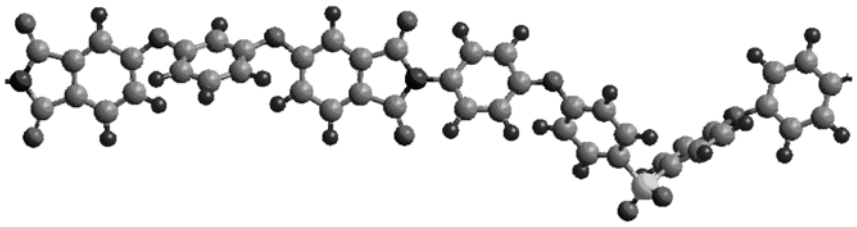

R-BAPB

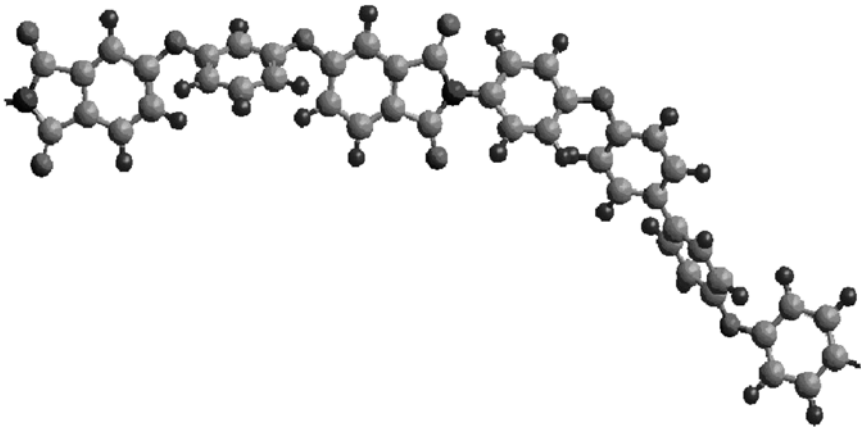

The persistence length was calculated through the following formula [24]:

$$a = \frac{1}{\langle l_i \rangle} \sum_{j=i}^{\infty} l_i^T \langle T_i T_{i+1} \ldots T_{j-1} \rangle l_j, \qquad (1)$$

where $l_i = \langle l_i \rangle \begin{pmatrix} 1 \\ 0 \\ 0 \end{pmatrix}$ and l_i^T is transposed l_i.

In Eq. (1), T_i is defined as

$$T_i = \begin{pmatrix} -\cos\theta_i & \sin\theta_i & 0 \\ -\sin\theta_i \cos\varphi_i & -\cos\theta_i \cos\varphi_i & -\sin\varphi_i \\ -\sin\theta_i \sin\varphi_i & -\cos\theta_i \sin\varphi_i & \cos\varphi_i \end{pmatrix}, \qquad (2)$$

where θ_i is the angle between the $i + 1$ and i bonds, around which rotation occurs, and φ_i is the torsion angle of the i bond ($\varphi_i = 180°$ corresponds to the trans conformation).

The virtual bonds for two PI molecules were determined as shown below.

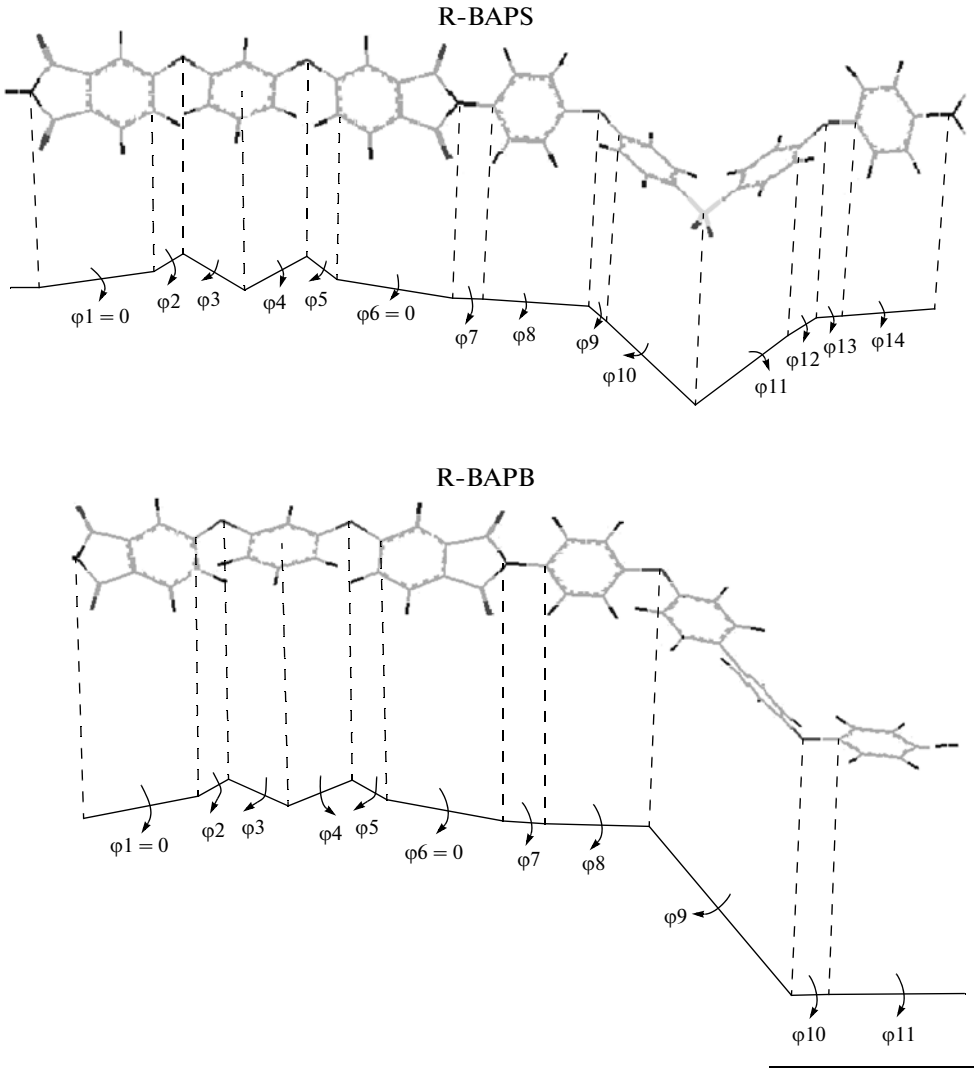

The bond lengths and valence angles were assumed to be constant. Their values were derived from the data on conformations of molecular fragments consisting of two repeating units (Tables 3 and 4) and calculated via the AM1 semi-empirical quantum-chemistry method.

Table 4. Virtual-bond lengths and valence angles in R-BAPB

i	1	2	3	4	5	6	7	8	9	10	11
l	4.67	1.39	2.79	2.79	1.39	4.67	1.41	4.19	9.81	1.39	4.21
θ°	154.3	117.2	120	117.2	154.3	171.2	177.4	123.7	121.16	173.6	171.4

Table 5. The lengths of persistence vectors for R-BAPS

i	0	1	2	3	4	5	6	7	8	9	10	11	12	13
a_i, Å	12.7	8.9	4.7	7.3	9.1	13.7	14.4	9.9	8.5	8.3	6.9	12.3	7.8	14.1

Note: The mean length $\langle a_i \rangle = 9.9$ Å.

Table 6. Persistence-vector lengths for R-BAPB

i	0	1	2	3	4	5	6	7	8	9	10
a_i, Å	13.1	9.4	5.2	8.3	11.1	18.1	19.7	15.2	13.8	17.3	14.4

Note: The mean length is $\langle a_i \rangle = 13.2$ Å.

For the polymer chain with independent rotations around neighboring bonds, the mean product of matrices in formula (1) is the product of averaged matrices:

$$\langle T_i T_{i+1} \ldots T_{j-1} \rangle = \langle T_i \rangle \langle T_{i+1} \rangle \ldots \langle T_{j-1} \rangle \quad (3)$$

It follows from the symmetry condition for all the bonds that $\langle \sin \varphi_i \rangle = 0$. Then, the transition matrix appears as follows:

$$\langle T_i \rangle = \begin{pmatrix} -\cos\theta_i & \sin\theta_i & 0 \\ -\sin\theta_i \langle \cos\varphi_i \rangle & -\cos\theta_i \langle \cos\varphi_i \rangle & 0 \\ 0 & 0 & \langle \cos\varphi_i \rangle \end{pmatrix} \quad (4)$$

If rotations around certain neighboring bonds (n and $n + 1$ bonds) are interdependent, the calculation procedure is different:

$$\langle T_i T_{i+1} \ldots T_{j-1} \rangle = \langle T_i \rangle \langle T_{i+1} \rangle \ldots \langle T_n T_{n+1} \rangle \ldots \langle T_{j-1} \rangle \quad (5)$$

In order to obtain the mean values, it is necessary to know the statistical weight matrix that can be derived from the calculated data on conformational energy as a function of internal rotation angles.

The persistence lengths of R-BAPS and R-BAPB polyimides were calculated under the assumption that rotations around bonds are free and independent.

The value of the persistence length calculated through formula (1) depends on the choice of initial bond i. If the zero bond (bond 14 for the first polymer and bond 12 for the second polymer that are statistically equivalent to the zero bonds due to chemical periodicity) is taken as the initial one, the persistence-length vector (the persistence vector), for example, for R-BAPS in case of independent rotations, is determined via the following relationship:

$$\begin{aligned} a_0 &= l_0 + \langle T_0 \rangle l_1 + \langle T_0 \rangle \langle T_1 \rangle l_2 + \ldots + \langle T_0 \rangle \ldots \langle T_{12} \rangle l_{13} \\ &+ \langle T_0 \rangle \ldots \langle T_{13} \rangle (l_0 + T_0) l_1 + \langle T_0 \rangle \langle T_1 \rangle l_2 \\ &+ \ldots + \langle T_0 \rangle \ldots \langle T_{12} \rangle l_{13}) + \ldots \\ &= (E + M_0 + M_0^2 + \ldots) L_0, \end{aligned} \quad (6)$$

where $M_0 = \langle T_0 \rangle \langle T_1 \rangle \langle T_2 \rangle \langle T_3 \rangle \langle T_4 \rangle \langle T_5 \rangle \langle T_6 \rangle \langle T_7 \rangle \langle T_8 \rangle \langle T_9 \rangle \times \langle T_{10} \rangle \langle T_{11} \rangle \langle T_{12} \rangle \langle T_{13} \rangle$ and $L_0 = l_0 + \langle T_0 \rangle l_1 + \langle T_0 \rangle \langle T_1 \rangle l_2 + \ldots + \langle T_0 \rangle \ldots \langle T_{12} \rangle l_{13}$. M_0 and L_0 are determined as the effective transformation matrix and the effective binding vector, respectively; and E is the unit matrix.

If the first bond is used as the initial bond, the calculation procedure is similar:

$$\begin{aligned} a_1 &= (E + M_1 + M_1^2 + \ldots) L_1 \\ M_1 &= \langle T_1 \rangle \langle T_2 \rangle \langle T_3 \rangle \langle T_4 \rangle \langle T_5 \rangle \langle T_6 \rangle \langle T_7 \rangle \langle T_8 \rangle \langle T_9 \rangle \langle T_{10} \rangle \\ &\times \langle T_{11} \rangle \langle T_{12} \rangle \langle T_{13} \rangle \langle T_0 \rangle \\ L_1 &= l_1 + \langle T_1 \rangle l_2 + \langle T_1 \rangle \langle T_2 \rangle l_3 + \ldots + \langle T_1 \rangle \ldots \langle T_{13} \rangle l_0 \end{aligned} \quad (7)$$

The calculated data are listed in Tables 5 and 6.

Allowance for the relationship between rotations the around the near-hinge bonds resulted in a certain gain in their persistence lengths. This gain is equal for both PIs. In both cases, the correction is less than 1 Å.

Thus, the above data make it possible to conclude that R-BAPB and R-BAPS polyimides possess almost the same flexibilities, while insertion of the SO_2 hinge group into the diamine fragment results only in an insignificant increase in the flexibility of R-BAPS relative to that of R-BAPB (~20%).

As follows from the structure of the repeating unit, the presence of sulfur and oxygen heteroatoms in the diamine component of EXTEM® cannot cause a reduction in the persistence length of EXTEM® relative to that of ULTEM® but facilitates a noticeable change in physical characteristics. The character of these changes is identical for the ULTEM®–EXTEM® and R-BARB–R-BAPS pairs.

Therefore, the alteration of physical characteristics of PIs during insertion of the SO_2 hinge group containing sulfur and oxygen heteroatoms into the diamine fragment is most likely not associated with a change in the flexibility of the polymer chain.

ALL-ATOM COMPUTER SIMULATION

An all-atom computer simulation using the Gromacs software package was performed in order to elucidate what factor determines the difference between the thermophysical and mechanical parameters of R-BAPB and R-BAPS [25, 26].

The model block samples of R-BAPB and R-BAPS are cubic cells with periodic boundary conditions. A cell contains 27 polymer chains consisting of 8 repeating units. Hydrogen atoms are linked to chain ends. The systems under consideration have the following parameters.

Polymer	R-BARB	R-BAPS
Number of repeating units per chain	8	8
Number of atoms in the chain consisting of eight repeating units	658	682
Number of chains in the system	27	27
Number of atoms in the system	17766	18414

As was shown in [19], the critical number-average molecular mass, at which the transition from the oligomer to the polymer is observed, is $M_n \sim 6000 \sim 6000$. (This value corresponds to weight-average molecular mass $M_w \sim 18\,000$ at a polydispersity of ~3; at this number-average molecular mass, the character of the dependence of viscosity on M_w changes.) This circumstance determined the selection of the degree of polymerization of macromolecules during simulation.

The Gromos 53a6 force field was used to describe interactions in the system [27]. The potential energy of the system in this case is composed of the energy of bond expansion, the energy of deformation of valence and torsion angles, and the terms for bulk and electrostatic interactions. The LINCS algorithm [28] was used to maintain the specified bond lengths, valence and torsion

angles; the PME method [29, 30] was used to allow for electrostatic interactions. During calculation of electrostatic interactions, the cutoff radius for electrostatic interactions, r_C, in the real space was set to 1 nm, while the lattice increment for summing in the Fourier space was taken to be 0.12 nm. Partial charges of atoms in monomeric units were calculated through the AM1 semi-empirical method [31–33].

The simulation was performed in the NPT ensemble. A Berendsen thermostat and a Berendsen barostat with time constants of $\tau_T = 0.1$ ps and $\tau_p = 0.5$ ps, respectively, were used to maintain a constant temperature and a constant average pressure in the system [34].

Note that the calculated characteristics of block PIs depended on the initial configuration. Under certain initial conditions, it was difficult to mix polymer chains; therefore, the simulated samples were much different from the experimental amorphous samples. The maximum degree of mixing was achieved via the following method for formation of the initial configuration of polymer matrices. A partially folded conformation (mace-shaped) was selected as the initial conformation of the PI molecule. The genconf software (the Gromacs software package) was used to almost equidistantly place 27 of these molecules into a sufficiently large cubic cell. Each polymer chain was rotated in space by a randomly selected angle. The cell volume was selected so that the chains did not overlap during generation of the initial configuration. The generated systems were subsequently equilibrated via several stages. The initial configuration of a single molecule of R-BAPS and the cell composted of these molecules prior to compression are shown below as an example.

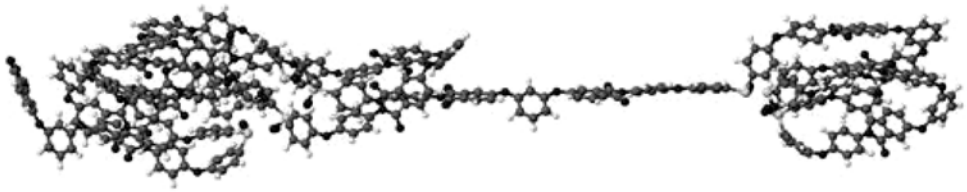

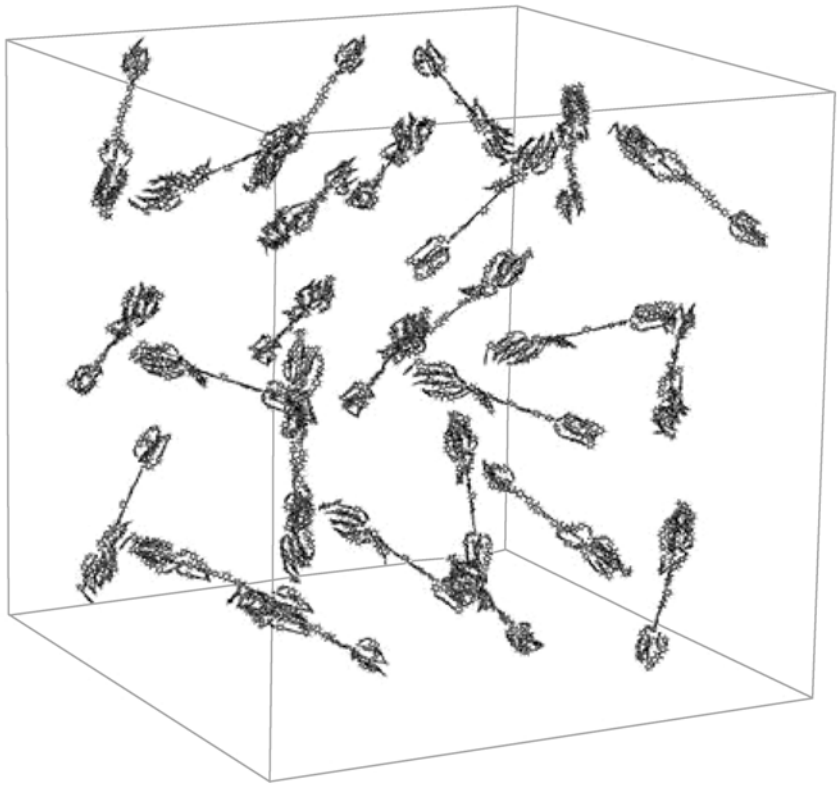

The system with the rarefied polymer was subjected to compression through a gradual increase in pressure. During the first simulation series for 1 ns, the system was simulated at an average pressure of 50 bar. The subsequent simulation was conducted at 150 bar for 2 ns and at 300 bar for 7 ns. The pressure was then

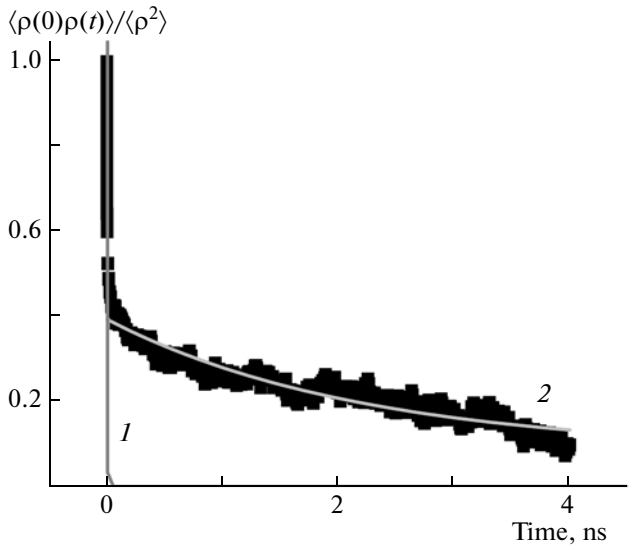

Fig. 1. Time dependence of autocorrelation function of density $C_\rho(t)$ of the R-BAPS sample at 600 K. The calculated relaxation times are (*1*) $\tau_1 \sim 0.0015$ and (*2*) $\tau_2 \sim 2.2$ ns.

reduced, and the system was simulated for 5 ns at an average pressure of 150 bar. Finally, the system was simulated for 5 ns at a pressure of 1 bar. After compression (the total duration was 20 ns), the polymer annealing was conducted by analogy with [35]. During annealing, the temperature was gradually decreased from $T_{max} = 600$ K to $T_{min} = 290$ K with an increment of 50 K. The maximum annealing temperature was selected under the assumption that it is higher than the glass-transition temperature by ~100 K (an even higher increase in T_{max} complicates the simulation of the system because thermal degradation of the sample becomes possible), when the glass-transition temperature is independent of T_{max} [36]. After each variation in temperature, the system was simulated for 2 ns. When the temperature of the system was reduced to T_{min}, the stepwise heating of the system to T_{max} was performed. During the annealing, the cooling–heating cycle was repeated three times. The total duration of the annealing was 78 ns; the total duration of the entire procedure of generation of the initial simulation cell was 98 ns. After completion of annealing, the sam-

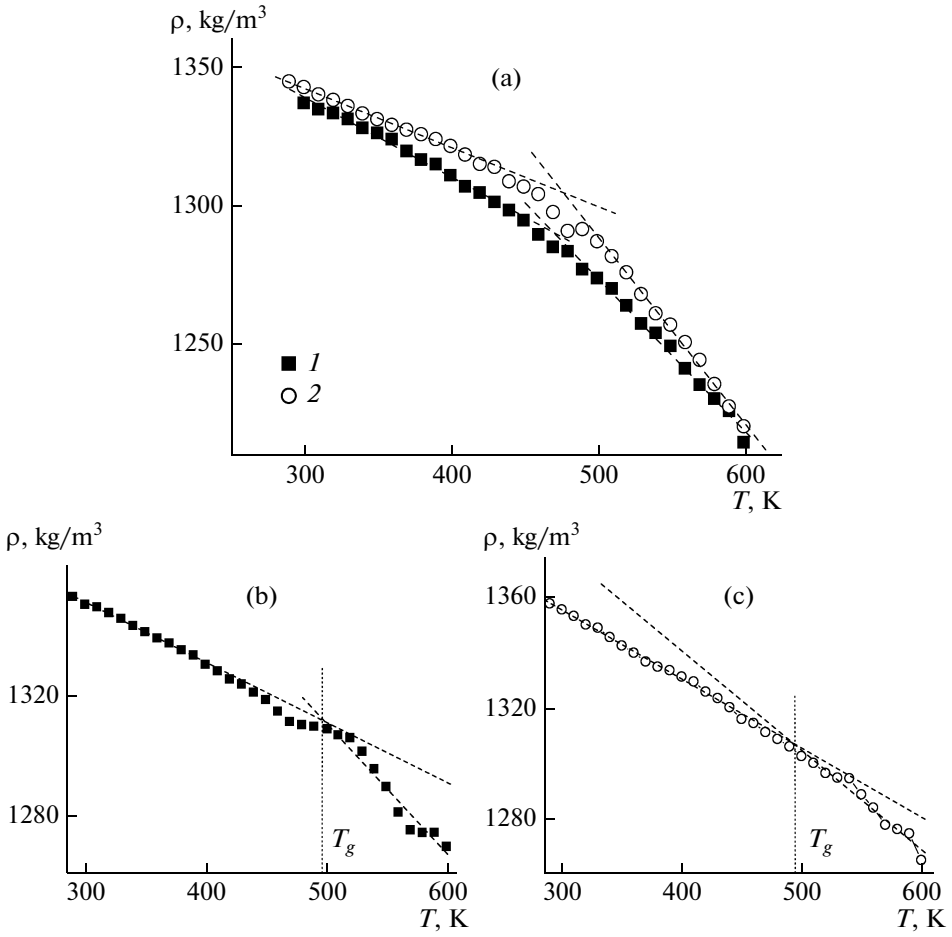

Fig. 2. Temperature dependence of block PI samples during cooling at rates of γ = (*1*) 5×10^{-3} K/ps and (*2*) 5×10^{-4} K/ps for (a) R-BAPB and (b, c) R-BAPS; T_g = (b) 496 and (c) 494 K.

ple was simulated for another 10 ns at 600 K. After that, the system was considered to be equilibrated. (The total simulation time from the initial configuration of the system to the final configuration was 108 ns.)

In order to assess the characteristic time required to attain the equilibrium state of the system, autocorrelation functions $C_\rho(t)$ of the density of the system were calculated:

$$C_\rho(t) = \frac{\langle \rho(0)\rho(t)\rangle}{\langle \rho^2 \rangle}, \quad (8)$$

where $\rho(t)$ is the density of the system at time t and $\langle \rho^2 \rangle$ is the average density of the system during simulation.

An analysis of the time dependence of the autocorrelation function showed that, for density fluctuations of the PI block samples, two relaxation processes were observed with characteristic times of ~1.5 ps and 2–5 ns, respectively. (In Fig. 1, the $C_\rho(t)$ dependence for the R-BAPS sample at 600 K is shown as an example.) Thus, the total time of system equilibration was two orders of magnitude higher than the maximum characteristic time of density fluctuation. This finding makes it possible to consider that the resulting samples are equilibrated and to use them as initial configurations for further simulation and calculation of the glass-transition temperature and the volumetric-expansion coefficients.

RESULTS AND DISCUSSION

Glass-Transition Temperature

In order to calculate glass-transition temperatures T_g of block samples of the R-BAPB and R-BAPS polyimides, they were cooled from the temperature of 600 K, at which PIs are in the plastic state. In order to gain insight into the effect of the rate of cooling on the glass-transition temperature, the equilibrated polymer melt was gradually cooled at two rates differing by an order of magnitude. The temperature was successively reduced by 10 K at each stage, and the polymer was equilibrated prior to the subsequent reduction in temperature for 2 or 20 ns. These values correspond to effective cooling rates of $\gamma = 5 \times 10^{-3}$ K/ps and $\gamma = 5 \times 10^{-4}$ K/ps, respectively. The temperature dependence of the average density of the samples at each cooling step is shown in Fig. 2. The resulting dependences contain two regions where the density is directly proportional to temperature. At low temperatures, the linear region corresponds to the glassy state of PIs, whereas at higher temperatures, it corresponds to the melt. The point of intersection of the lines obtained through approximation of linear regions via the least-squares method corresponds to T_g at a certain cooling rate.

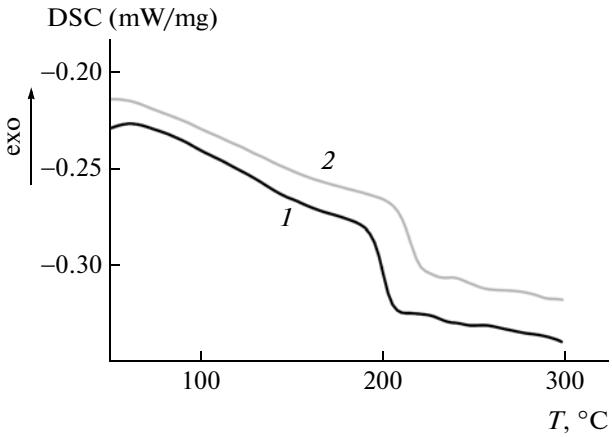

Fig. 3. The experimental DSC data used to determine the glass-transition temperatures of (*1*) R-BAPB and (*2*) R-BAPS polyimides; $M \sim 30 \times 10^3$ g/mol, and T_g= (*1*) 199.3 and (*2*) 213.5°C.

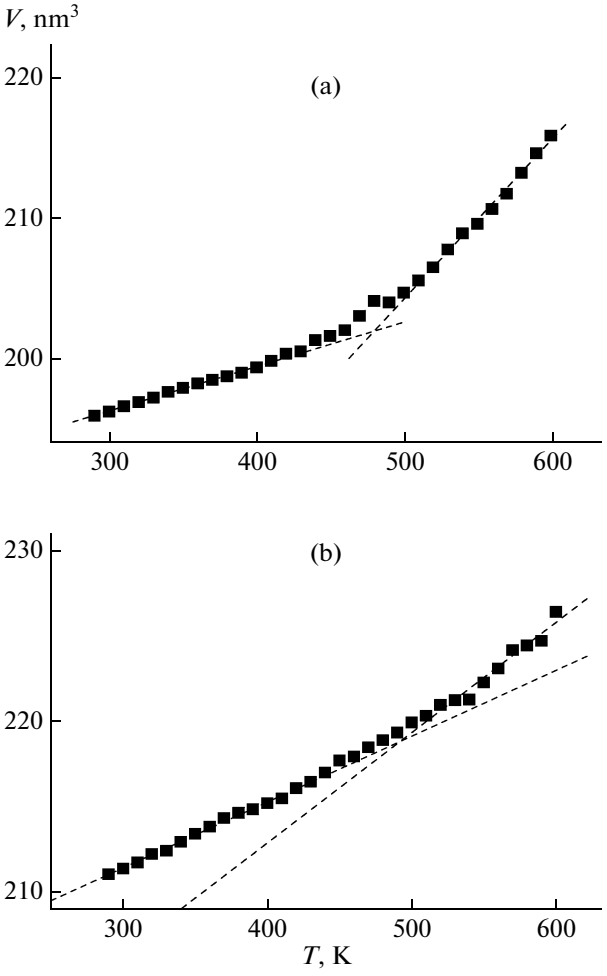

Fig. 4. Temperature dependences of the volume of the block PI sample according to computer-simulation data (the cooling rate $\gamma = 5 \times 10^{-4}$ K/ps) for (a) R-BAPB and (b) R-BAPS.

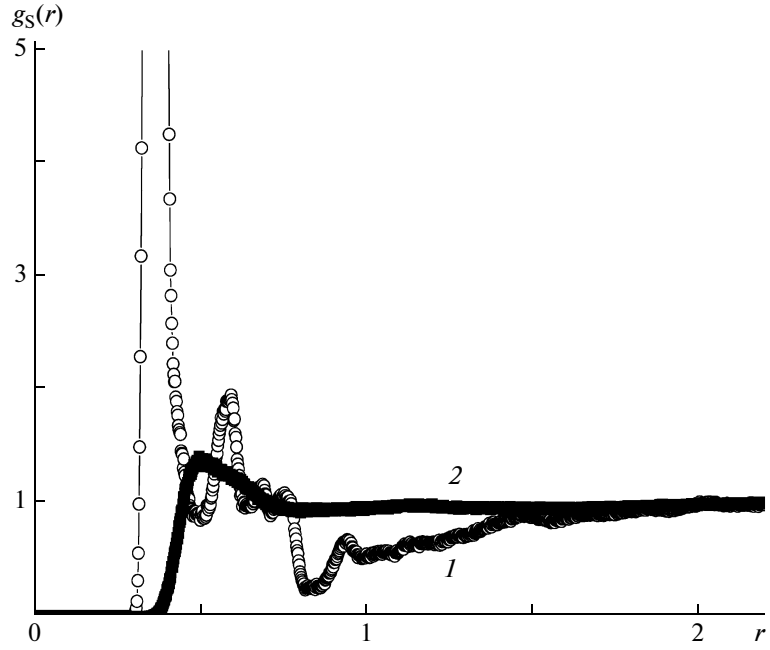

Fig. 5. Pairwise radial distribution function $g_S(r)$ of sulphur atoms at 600 K for (*1*) R-BAPS and (*2*) R-BAPS^{neutr} samples.

The calculated glass-transition temperatures are given below for both PIs at two cooling rates. In order to estimate the error in determining T_g, a linear approximation was performed above and below the glass-transition temperature with the use of various numbers of points. The following values of T_g were obtained.

Method of determining T_g	R-BAPB, K	R-BAPS, K
Simulation at a cooling rate of 5×10^{-3} K/ps	471 ± 2	496 ± 3
Simulation at a cooling rate of 5×10^{-4} K/ps	475 ± 2	494 ± 3
Experimental values based on the DSC data	472.5	486.7
QSPR values obtained on the basis of the QSPR analysis	468.7	516.4

Table 7. Volumetric-thermal-expansion coefficients β for block samples of R-BAPB and R-BAPS polyimides

Polymer	β value, K^{-1}		
	Glassy state		Melt (computer simulation)
	QSPR analysis	Computer simulation	
R-BAPB	2.111×10^{-4}	1.63×10^{-4}	5.49×10^{-4}
R-BAPS	1.928×10^{-4}	1.81×10^{-4}	2.92×10^{-4}

The data obtained are in good agreement with those obtained in [22] for R-BAPB ($T_g = 477$ K) and R-BAPS ($T_g = 490$ K) as well as with the recent experimental data based on DSC results (for samples with $M_n \sim 15\,000$ g/mol, which is higher than M_w of the polymers investigated via computer simulation; Fig. 3).

The glass-transition temperature of a polymer is known to depend on the rate of cooling. The relationship between these parameters is determined by the following equation [37–39]:

$$T_g(\gamma) = T_0 - \frac{B}{\log(A\gamma)}, \quad (9)$$

where T_0 is the glass-transition temperature at an infinitely low cooling rate and A and B are empirically determined coefficients.

In our case, the T_g values obtained at different cooling rates differ slightly (within the limits of error). Meanwhile, the value calculated on the basis of the results of simulation of T_g is in good agreement with the experimental data presumably because, for the investigated systems, the second item in Eq. (9) is small and changes insignificantly with the cooling rate. Similar results were obtained for BPDA/134APB polyimides, for which the T_g values obtained for a cooling rate much higher than the experimental cooling rate coincided with the experimental data [35].

Thermal-Expansion Coefficients Above and Below the Glass-Transition Temperature

Volumetric-thermal-expansion coefficients β of PIs in the glassy and melted states were calculated through the following relationship:

$$\beta = \frac{1}{V}\left(\frac{dV}{dT}\right)_p, \qquad (10)$$

where V is the sample volume and $(dV/dT)_p$ is the change in the volume of the system after heating by dT degrees at a constant pressure. Changes in the volume of the sample after temperature variation were determined from the slope of linear regions of temperature dependences of the volume of the sample obtained during simulation (Fig. 4). Volume V in Eq. (10) corresponds to the volume of the system at the initial point (at the minimum temperature) of the corresponding linear regions. The calculation results are listed in Table 7. Coefficients β for the both PIs in the glassy state are in close agreement with the data calculated via the QSPR method (Table 1).

Thus, the results of the computer simulation are in agreement with the available experimental data and the QSPR analysis, whereas the values of the glass-transition temperature obtained via simulation describe the experimental data with a higher accuracy than the results of the QSPR analysis.

Association of S and O Heteroatoms in the Sulfone Group

In order to understand the molecular mechanism of variation in the properties of PIs after insertion of the SO_2 hinge group into the diamine component of PI, the distribution of sulfur and oxygen atoms in this group over the PI sample was studied. The image of a typical instantaneous configuration of the R-BAPS sample at 600 K obtained through computer simulation is shown in Fig. 4a. Because the partial charges of sulfur and oxygen within the SO_2 group are higher than those of the remaining atoms, i.e., $Q_S = 2.9$ and $Q_O = -0.94$ (the situation may be different if partial charges are calculated through another method), these atoms tend to form associates, which can be clearly identified in the images of typical instantaneous configurations of R-BAPS and R-BAPS^{neutr} samples at 600 K (see below). Light gray and dark gray balls represent sulfur and oxygen atoms within the SO_2 group.

R-BAPS

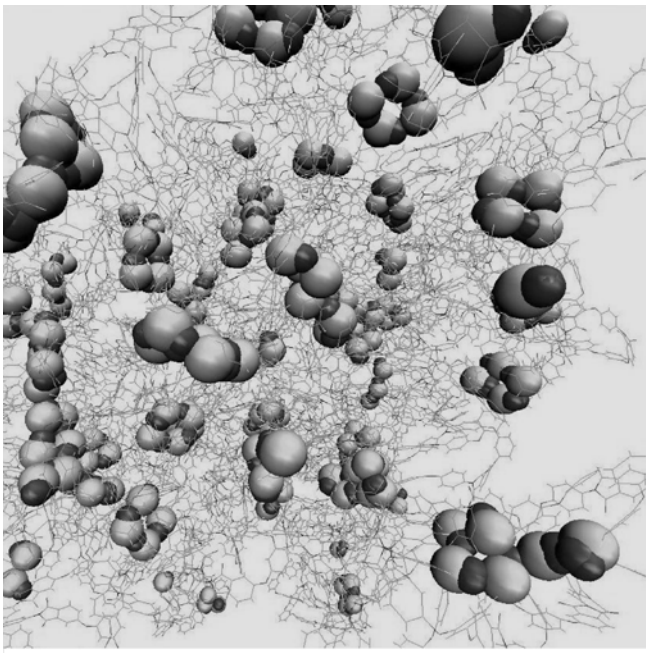

R-BAPS^{neutr}

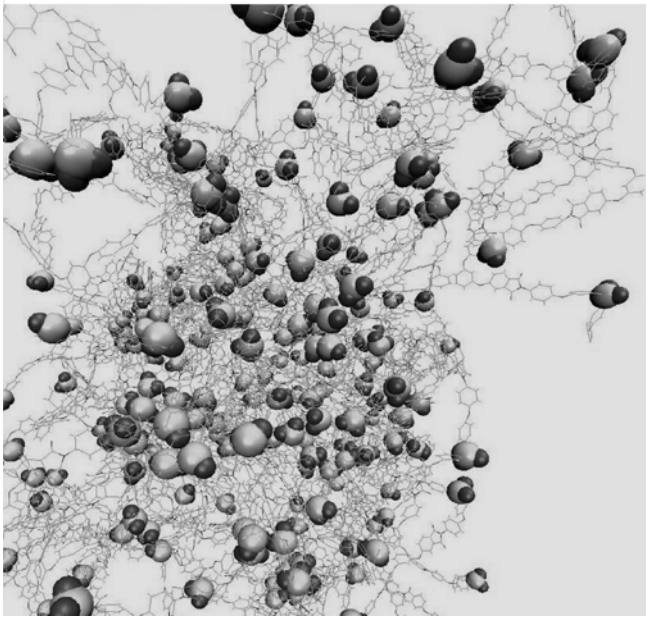

In order to confirm that electrostatic interactions between sulfur and oxygen atoms are responsible for the observed change in the properties of PIs after insertion of the SO_2 hinge group, an additional simulation of the R-BAPS block sample was performed at zero values of partial charges on all the atoms. The R-BAPS^{neutr} sample was newly generated through the procedure described above for charged R-BAPB and R-BAPS samples. No associates composed of sulfur and oxygen atoms that are related to the presence of SO_2, groups in the R-BAPS^{neutr} sample were observed in the images.

Thus, in order to confirm the presence of associating sulfone groups in the R-BAPS sample and their absence in the R-BAPS^{neutr} sample, pairwise distribution functions $g_S(r)$ for sulfur atoms were calculated. The value of the $g_S(r)$ function is associated with the probability of finding a sulfur atom at distance r from another sulfur atom. The appearance of pairwise distribution functions $g_S(r)$ in the R-BAPS and R-BAPS^{neutr} samples (Fig. 5) attests to the existence of these associates. The pattern of correlation function $g_S(r)$ in the absence of partial charges for the R-BAPS^{neutr} sample is typical of the melts and is characterized by a single maximum. In the presence of partial charges, the first maximum of correlation function $g_S(r)$ shifts toward lower values and is sharper. Moreover, the next maxima emerge.

CONCLUSIONS

The theoretical and experimental studies and all-atom computer simulation of the block samples of R-BAPB and R-BAPS polyimides has shown that the presence of the sulfone group in the diamine component of the repeating unit of the R-BAPS polyimide holds significance. The QSPR analysis turned out to be an efficient tool for the qualitative prediction of comparative variation in the properties of PIs in the glassy state after insertion of the sulfone group into the diamine component of the repeating unit. The all-atom computer simulation using the molecular dynamics method makes it possible not only to calculate the glass-transition temperature and the coefficients of volumetric thermal expansion of the block PI samples, which are in good agreement with the available data, but also to propose the molecular mechanism determining changes in the properties of PIs after modification of the diamine fragment of the repeating unit with the sulfone group.

The computer simulation in this study was performed with the use of the resources of the computer cluster of the Institute of Macromolecular Compounds, Russian Academy of Sciences, and the Chebyshev and Lomonosov supercomputers at Moscow State University. The QSPR analysis was performed with the Material Studio 5.5 software package at the Computer Research Center of Moscow State University.

REFERENCES

1. *Polyimides: A Class of Thermally Stable Polymers*, Ed. by M. I. Bessonov (Nauka, Leningrad, 1983) [in Russian].
2. I. W. Serfaty, Eng. Thermoplast. Prop. Appl., No. 4, 283 (1985).
3. W. Sederel, Kunststoffe **76**, 905 (1986).
4. A. L. Rusanov and G. S. Matvelashvili, Plast. Massy, No. 11, 3 (1991).
5. D. Heath and J. Wirth, US Patent No. 3,847,867 (1974).
6. D. E. Florian and I. W. Serfaty, Mod. Plast. Int. **12** (6), 38 (1982).
7. Y. Wang, L. Y. Jiang, T. Matsuurac, T. S. Chung, and S. H. Goh, J. Membr. Sci. **318**, 217 (2008).
8. N. Peng, T. S. Chung, M. L. Chng, and W. Aw, J. Membr. Sci. **360**, 48 (2010).
9. J. Xia, S. Liu, P. K. Pallathadka, M. L. Chng, and T. S. Chung, Ind. Eng. Chem. Res. **49**, 12014 (2010).
10. C. J. Lee, J. Macromol. Sci., Rev. Macromol. Chem. **29**, 431 (1989).
11. J. Bicerano, *Prediction of Polymer Properties* (Marcel Dekker, New York, 2002).
12. V. M. Svetlichnyi and V. V. Kudryavtsev, Polymer Science, Ser. B **45**, 140 (2003) [Vysokomol. Soedin., Ser. B **45**, 56 (2003)].
13. V. E. Yudin, V. M. Svetlichnyi, G. N. Gubanova, A. I. Grigor'ev, T. E. Sukhanova, I. V. Gofman, A. L. Didenko, E. N. Popova, R. N. Fedorova, and V. V. Kudryavtsev, Polymer Science, Ser. A **44**, 148 (2002) [Vysokomol. Soedin., Ser. A **44**, 257 (2002)].
14. V. E. Yudin, V. M. Svetlichnyi, G. N. Gubanova, A. L. Didenko, T. E. Sukhanova, V. V. Kudryavtsev, S. Ratner, and G. Marom, J. Appl. Polym. Sci. **83**, 2873 (2002).
15. V. E. Yudin, V. M. Svetlichnyi, A. N. Shumakov, D. G. Letenko, A. Y. Feldman, G. Marom, Macromol. Rapid Commun. **26**, 885 (2005).
16. V. E. Yudin, A. Y. Feldman, V. M. Svetlichnyi, A. N. Shumakov, and G. Marom, Compos. Sci. Technol. **67**, 789 (2007).
17. V. E. Yudin, J. U. Otaigbe, L. T. Drzal, and V. M. Svetlichnyi, Adv. Compos. Lett. **15** (4), 137 (2006).
18. A. N. Shumakov, V. E. Yudin, V. M. Svetlichnyi, A. N. Didenko, N. N. Bogorad, E. N. Popova, D. G. Letenko, Yu. A. Fadin, and A. N. Solov'ev, Vopr. Materialoved. **46**, 158 (2006).
19. V. E. Yudin, G. M. Divoux, J. U. Otaigbe, and V. M. Svetlichnyi, Polymer **46**, 10866 (2005).
20. V. E. Yudin, V. M. Svetlichnyi, A. N. Shumakov, R. Schechter, H. Harel, and G. Marom, Composites A **39**, 85 (2008).
21. T. Kurose, V. E. Yudin, J. U. Otaigbe, and V. M. Svetlichnyi, Polymer **48**, 7130 (2007).
22. V. E. Yudin and V. M. Svetlichnyi, RZhKh **53** (4), 75 (2009).
23. T. M. Birshtein, Vysokomol. Soedin., Ser. A **19**, 54 (1977).
24. P. J. Flory, *Statistical Mechanics of Chain Molecules* (Wiley, New York, 1969; Mir, Moscow, 1971).
25. B. Hess, C. Kutzner, D. Van der Spoel, and E. Lindahl, J. Chem. Theory Comput. **4**, 435 (2008).
26. D. Van der Spoel, E. Lindahl, B. Hess, G. Groenhoff, A. E. Mark, and H. J. C. Berendsen, J. Comput. Chem. **26**, 1701 (2005).
27. C. Oostenbrink, A. Villa, A. E. Mark, and W. F. Van Gunsteren, J. Comput. Chem. **25**, 1656 (2004).
28. B. Hess, H. Bekker, H. J. C. Berendsen, and J. G. E. M. Fraaije, J. Comput. Chem. **18**, 1463 (1997).

29. T. Darden, D. York, and L. Pedersen, J. Chem. Phys. **98**, 10089 (1993).

30. U. Essmann, L. Perera, M. L. Berkowitz, T. Darden, H. Lee, and L. G. Pedersen, J. Chem. Phys. **103**, 8577 (1995).

31. J. P. P. Stewart, J. Comput. Chem. **10**, 209 (1989).

32. W. Thiel, in *Modern Methods and Algorithms of Quantum Chemistry*, Ed. by J. Grotendorst and J. von Neumann (Inst. for Computing, NIC Ser., Jülich, 2000), Vol. 1.

33. V. A. Basiuk, R. Navarro-González, Y. Benilan, and F. Raulin, Spectrochim. Acta, Part A **57**, 505 (2001).

34. H. J. C. Berendsen, in *Computer Simulations in Materials Science*, Ed. by M. Meyer and V. Pontikis (Kluwer, Dordrecht, 1991).

35. P. V. Komarov, Y.-T. Chiu, S.-M. Chen, and P. Reineker, Macromol. Theory Simul. **19**, 64 (2010).

36. J. L. Chung, J. Macromol. Sci., Rev. Macromol. Chem. Phys. **29**, 431 (1989).

37. R. Brüning and K. Samwer, Phys. Rev. B: Condens. Matter **46**, 11318 (1992).

38. K. Vollmayr, W. Kob, and K. Binder, J. Chem. Phys. **105**, 4714 (1996).

39. A. V. Lyulin, N. K. Balabaev, and M. A. J. Michels, Macromolecules **36**, 8574 (2003).